FE analysis of RC structures using DSC model with yield surfaces for tension and compression

A.H. Akhaveissy[*1], C.S. Desai[2], D. Mostofinejad[3] and A. Vafai[4]

[1]*Department of Civil Engineering, Faculty Engineering, Razi University, P.O. Box: 67149–67346,
Kermanshah, Iran*
[2]*Department of Civil Engineering and Engineering Mechanics, University of Arizona, Tucson, AZ 85721, U.S.A.*
[3]*Department of Civil Engineering, Isfahan University of Technology, Isfahan-Iran*
[4]*Department of Civil Engineering, Sharif University of Technology, Tehran-Iran*

Abstract. The nonlinear finite element method with eight noded isoparametric quadrilateral element for concrete and two noded element for reinforcement is used for the prediction of the behavior of reinforcement concrete structures. The disturbed state concept (DSC) including the hierarchical single surface (HISS) plasticity model with associated flow rule with modifications is used to characterize the constitutive behavior of concrete both in compression and in tension which is named DSC/HISS-CT. The HISS model is applied to shows the plastic behavior of concrete, and DSC for microcracking, fracture and softening simulations of concrete. It should be noted that the DSC expresses the behavior of a material element as a mixture of two interacting components and can include both softening and stiffening, while the classical damage approach assumes that cracks (damage) induced in a material treated acts as a void, with no strength. The DSC/HISS-CT is a unified model with different mechanism, which expresses the observed behavior in terms of interacting behavior of components; thus the mechanism in the DSC is much different than that of the damage model, which is based on physical cracks which has no strength and interaction with the undamaged part. This is the first time the DSC/HISS-CT model, with the capacity to account for both compression and tension yields, is applied for concrete materials. The DSC model allows also for the characterization of non-associative behavior through the use of disturbance. Elastic perfectly plastic behavior is assumed for modeling of steel reinforcement. The DSC model is validated at two levels: (1) specimen and (2) practical boundary value problem. For the specimen level, the predictions are obtained by the integration of the incremental constitutive relations. The FE procedure with DSC/HISS-CT model is used to obtain predictions for practical boundary value problems. Based on the comparisons between DSC/HISS-CT predictions, test data and ANSYS software predictions, it is found that the model provides highly satisfactory predictions. The model allows computation of microcracking during deformation leading to the fracture and failure; in the model, the critical disturbance, D_c, identifies fracture and failure.

Keywords: Reinforced concrete; cracks; fracture; tension-compression behavior; disturbed state concept; plasticity; finite element analysis; softening behavior; validations

1. Introduction

*Corresponding author, Ph.D., E-mail: Ahakhaveissy@razi.ac.ir

The finite element method is commonly used for the analysis of reinforced concrete structures. Different constitutive models have been used to characterize behavior of concrete. Willam and Warnke (1974) developed a plasticity model for the triaxial failure surface for unconfined behavior of plain concrete, and reported that the predictions compared well with the observed results of concrete failure. Bazant and Shieh (1978) used endochronic model for nonlinear triaxial behavior of concrete and predicted softening behavior of concrete under compression loading. Cervera *et al.* (1987) adopted a yield function depending only on first and second stress invariants, but they did not consider softening behavior of concrete in compression. An exponential function was used to simulate softening behavior of concrete in tension, and a softening parameter was used depending on the needed fracture energy to separate two crack surfaces. Predictions from their model compared well with observed results for reinforced concrete slab and beams. Carol *et al.* (1992) implemented a microplane model for concrete at element level for calculating compressive stresses.

The book by Willam and Tanabe (2001) contains a review of a collection of papers concerning finite element analysis of reinforced concrete structures; and various factors such as seismic behavior of structures, cyclic loading of reinforced concrete columns, and shear failure of reinforced concrete beams. Bazant and Luzio (2004) presented a nonlocal microplane model with strain-softening yield limits to analyze concrete structures using the finite element method; they considered strain localization in a concrete beam without bars.

A method for the integration of a class of plastic-damage material model was considered by Saritas and Filippou (2009); the Barcelona model was selected as the yield function. They analyzed beam A1 and A3 by Vecchio and Shim (2004). The predicted results by Saritas and Filippou (2009) are at good correlation with experimental data for beam A3 but not for the beam A1. Therefore, here the beam A1 is considered as one of examples.

In this paper, the disturbed state concept/hierarchical single surface (DSC/HISS) model is modified to analyze reinforced concrete structures in which different HISS single surfaces are used for compressive and tensile behavior of concrete. The proposed model can be called DSC/HISS-CT, CT denoting compression and tension. However, it is noticeable that in the DSC model, the average or observed behavior is expressed in terms of behaviors of the material as a mixture of Relative Intact (RI) or continuum part, and Fully Adjusted (FA) part that allows for softening or degradation; the DSC can account also for healing or stiffening. Both RI and FA parts are coupled and with the disturbance function, contribute to the observed behavior, which can include degradation or healing. The DSC is a unified approach with a different base than the damage model that does not include interaction between damaged and undamaged parts. However, the classical damage approach assumes that cracks (damage) induced in a material treated act as a void, with no strength (Kachanov 1986). For simplicity, the DSC/HISS-CT model is referred to as DSC model in this paper. Details of DSC/HISS models are given by (Desai *et al.* 1986, Desai and Salami 1987, Desai and Toth 1996, Desai 2001, Salami and Desai 1990); a brief description is given below.

The DSC/HISS with single yield surface is a unified and hierarchical model that can be used to characterize elastic, plastic and creep deformations, microcracking leading fracture and failure, degradation or softening, and healing or strengthening. It has been used for a wide range of materials such as clays, sands, ceramic, metals, alloys and silicon, and interfaces and joints (Desai 2001). It has been implemented in nonlinear finite element procedures which are used to solve a wide range of engineering problems including two- and three-dimensional (Desai 2001, 2002, 2007), and cyclic loading (Desai 2001, Pradhan and Desai 2006, Shao and Desai 2000). Thus, the
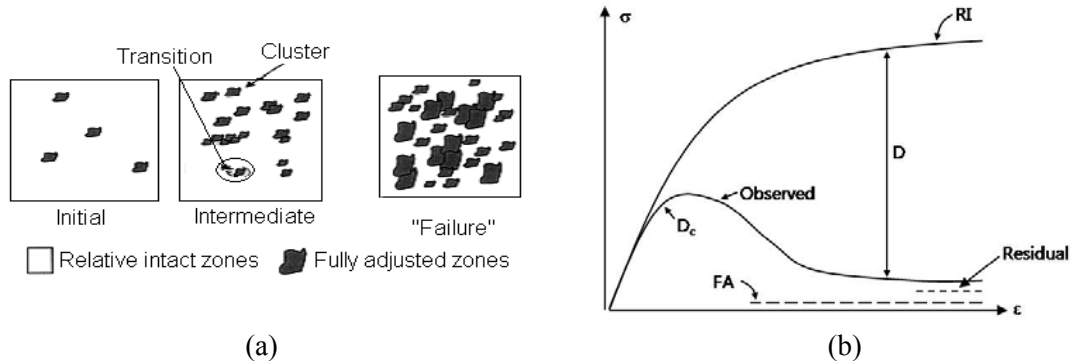
(a)   (b)

Fig. 1 (a) RI and FA states in DSC and (b) disturbance as coupling between RI and FA states

DSC model possesses a number of advantages compared to other available models that often account for only specific behavioral aspect(s).

The DSC/HISS models with single yield surface have also been used for modeling behavior of concrete and rocks (Desai and Salami 1987, Desai 2001, Salami and Desai 1990). In this paper, the DSC model is used for concrete in reinforced concrete structures with the new feature being the use of the HISS yield function for both yield in compression and tension.

2. Disturbed state concept with HISS model

The description of the DSC model herein is adopted from various publications, e.g. (Desai 2001). In this model, a deforming material element is assumed to be composed of two (or more) reference states, the relatively intact (RI), and the fully adjusted (FA), Fig. 1. The material is assumed to transform continuously from the relative intact (RI) state to the fully adjusted (FA) state, Fig. 1(a), at randomly distributed locations under external excitation such as mechanical and thermal loading. The transformation involves micro structural changes that cause particle reorientation and relative motions. The observed behavior is expressed in terms of that of RI and FA states using the disturbance function, D, which acts as a coupling or interaction mechanism between RI and FA states, Fig. 1(b); the disturbance grows as the material deforms and the plastic strain (or work) accumulates. Thus DSC includes the coupling intrinsically in which the micro cracked (damaged) or fully adjusted part also contributes to the response of the material. The RI and FA states can be defined by using various models. The continuum elasticity or plasticity can be used for modeling the response of RI state, while the FA state can be assumed to carry only hydrostatic stress or it can be modeled by using the critical state model (Desai 2001). Brief descriptions of the models for RI and FA states, and disturbance used in the DSC model, are given below.

2.1 Relative Intact (RI) state

The hierarchical single-surface (HISS) plasticity model (Desai *et al.* 1986) provides a general formulation for the elastoplastic characterization of the material behavior; it involves a *single* continuous yield surface compared to some previous models that involved multiple

(discontinuous) yield surfaces resulting in computational difficulties. This model, which can allow for isotropic and anisotropic hardening, and associated and non- associated plasticity characterizations, can be used to represent material response based on the continuum plasticity theory (Desai *et al.* 1986, Desai 2001). Usually, in the HISS model, the RI state is defined by using the associated plasticity; accordingly, the yield function, *F*, Fig. 2, is given by

$$F = \overline{J}_{2D} - (-\alpha \overline{J}_1^n + \gamma \overline{J}_1^2)(1 - \beta \, S_r)^{-0.5} = 0 \tag{1a}$$

$$\overline{J}_{2D} = {J_{2D}}\Big/{p_a}^2 \tag{1b}$$

$$\overline{J}_1 = (J_1 + 3R)/p_a \tag{1c}$$

$$S_r = \frac{\sqrt{27}}{2} \cdot \frac{J_{3D}}{J_{2D}^{1.5}} \tag{1d}$$

where, J_{3D} and J_{2D} third and second invariant of deviatoric stress tensor, respectively, J_1 first invariant of total stress tensor, p_a is the atmospheric pressure which is defined as 0.1013 MPa, *R* the reference stress used mainly to include the intercept ($\overline{c}$), which is proportional to cohesive strength Fig. 2, parameters γ and β are related to ultimate condition, and the hardening or growth function for the plastic yield can be expressed as

$$\alpha = \frac{a_1}{\xi^{\eta_1}} \tag{2}$$

where a_1 and η_1 are hardening parameters, and ξ is trajectory or accumulated plastic strains. Using *F*, Eq. (1a), the incremental stress-strain equations for RI (plasticity) model are derived as (Desai 2001)

$$d\sigma = \left[C^e - \frac{C^e\left(\dfrac{\partial Q}{\partial \sigma}\right)\left(\dfrac{\partial F}{\partial \sigma}\right)^T C^e}{\left(\dfrac{\partial F}{\partial \sigma}\right)^T C^e\left(\dfrac{\partial Q}{\partial \sigma}\right) - \dfrac{\partial F}{\partial \xi}\gamma_F} \right] d\varepsilon \tag{3a}$$

$$\gamma_F = \left[\left(\frac{\partial Q}{\partial \sigma}\right)^T \left(\frac{\partial Q}{\partial \sigma}\right) \right]^{1/2} \tag{3b}$$

σ = the stress vector, C^e = elastic constitutive matrix, *d* denotes increment and *Q* is the plastic potential function. When the associated flow rule is adopted, $F \equiv Q$.

For geologic materials and concrete, the compressive stress is assumed to be positive. The yield surface, *F*, Fig. 2, is valid for compressive behavior in the positive $J_1 - \sqrt{J_{2D}}$ space. Since the behaviors of material like concrete are different for compression and tension, the yield surface, Fig.
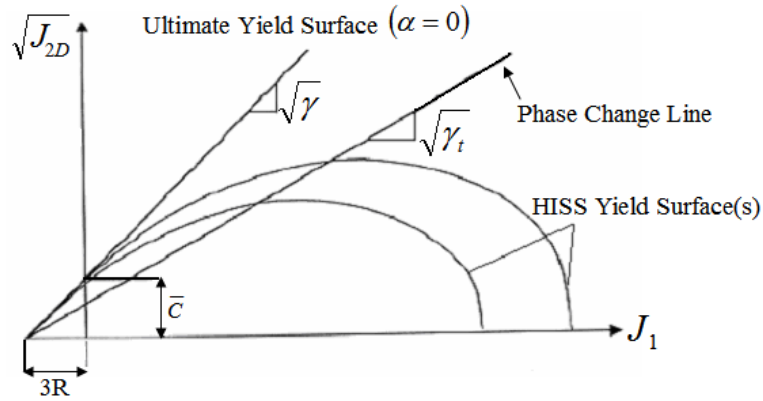
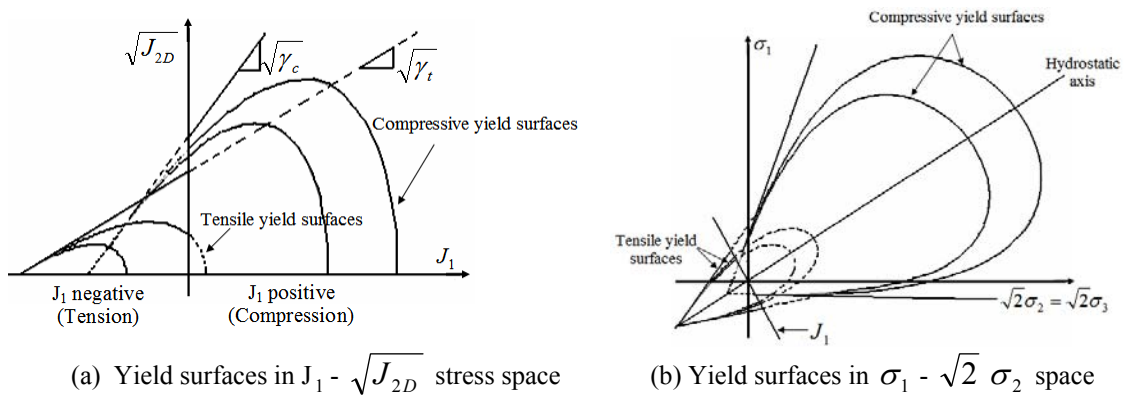Fig. 2 HISS yield surface in $J_1 - \sqrt{J_{2D}}$ space

(a) Yield surfaces in J_1 - $\sqrt{J_{2D}}$ stress space   (b) Yield surfaces in σ_1 - $\sqrt{2}\,\sigma_2$ space

Fig. 3 Schematic of compressive and tensile HISS yield surfaces (Desai 2007)

2, is not appropriate in the negative J_1-axis. Often, an ad hoc model such as stress transfer approach (Zienkiewicz *et al.* 1968) is used in which the computed tensile stress above the tensile strength is redistributed in the zone of the problem. The HISS model is used to simulate the material in the relative intact (continuum) state. The HISS model can be used for both compression and tension if material parameters are determined from appropriate laboratory tests under compression and tension. Such a model called DSC/HISS-CT, that can account for both compression and tension yield, has been introduced in (Desai 2007). However, DSC/HISS-CT is used for the first time in the study presented in this paper. Fig. 3 show yield surfaces for compression and tension.

2.2 Fully adjusted (FA) state

Various characterizations for the behavior of the FA state are given in (Desai 2001). In a simple form, the FA state for concrete can be considered by use of residual stress in the stress-strain

response, Fig. 1(b); fully adjusted stress can be also based on approximately 20% of compressive resistance of concrete in uniaxial test.

2.2.1 Disturbance

Disturbance, D, can be defined in various ways in terms of measured stress, void ratio, pore water pressure and nondestructive properties such as P or S wave velocities (Desai 2001). In terms of stress, it is defined as

$$D = \frac{\sigma_i - \sigma_a}{\sigma_i - \sigma_c} \tag{4}$$

where σ_i, σ_a and σ_c are RI, observed and FA stress values, respectively. In order to introduce D in the DSC model (the later Eq. (6)) it needs to be expressed in a mathematical form in terms of a basic variable such as accumulated plastic strains or work. Hence, D in terms of the accumulated deviatoric plastic strains is expressed using the (Weibull 1951) type function

$$D = D_u[1 - \exp(-A\xi_D^Z)] \tag{5}$$

where D_u is the ultimate disturbance (often assumed to be unity), ξ_D trajectory of (deviatoric) plastic strains and A and Z are disturbance parameters. The parameters in Eq. (5) are determined on the basis of the values of the measured σ_a at various points in the stress-strain curve, Eq. (4), and the corresponding values of ξ_D (Desai 2001).

Variations of disturbance, D, for typical stress-strain behavior for peak stress = 32 MPa (see later Fig. 6) are shown in Fig. 4. In this figure, the value of critical disturbance, D_c, is assumed to occur at about 0.9, which represents the intersection of tangents to the upper part of the middle and ultimate zones, Fig. 4. The microcracking may start at about $0.3\sigma_p$ where σ_p is the peak stress, Fig. 6 (later), when the disturbance is about $D = 0.001$ for compression and about $D = 0.001$ for tension. Then microcracking grows and coalesce into cracks that lead to fracture or failure at the critical disturbance, $D_c = 0.9$ (Desai 2001). Thus D can be used as a measure for identifying the initiation and growth of microcracking (based on test data) leading to fracture and failure. For example, when the disturbance reaches $D_c = 0.9$ or higher values, fracture occurs and grows. In the finite element analysis, elements that reach this critical or higher value are identified after each load increment; thus the initiation and growth of fracture are provided progressively by the computer procedure. In later applications, contours of D are plotted based on the computer results, and cracking and fracture are related to the values and extent of the disturbance.

Both the RI and FA states contribute to the material response through disturbance (D) as the coupling function. Following DSC equations in the incremental form shows this coupling (Desai 2001)

$$d\sigma_{ij}^a = (1-D)d\sigma_{ij}^i + Dd\sigma_{ij}^c + dD(d\sigma_{ij}^c - d\sigma_{ij}^i) \tag{6}$$

where d denotes the increment or rate, and σ_{ij} is the stress tensor. The DSC model in this study is based on small strains; however, it can be modified for large strains, which will require use of appropriate expressions for large strains that would contain second order terms beyond the first
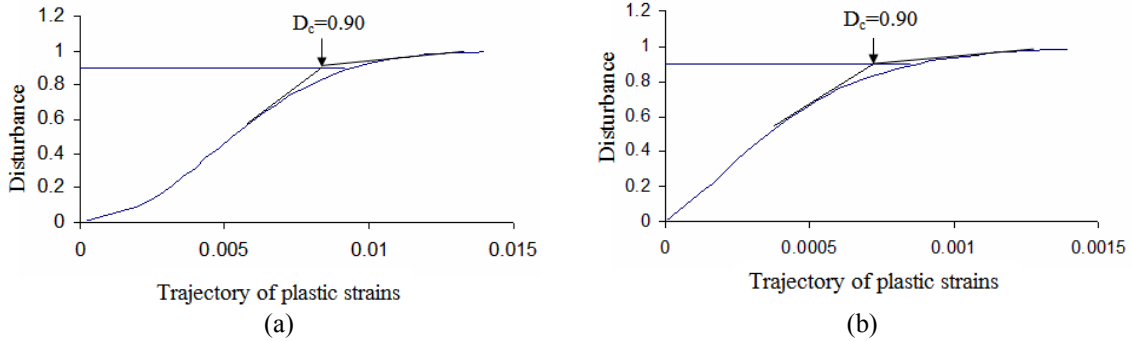
Fig. 4 Variation of *D* versus trajectory of plastic strains for 28-days concrete with compressive strength = 32 MPa for: (a) compression and (b) tension

derivative of displacement (Bathe 1996)

3. Numerical simulation of reinforced concrete structures behavior

3.1 Laboratory tests (Fig. 5)

Based on a number of tests for concrete, the following mathematical equations have been used by (Assan 2002, Coronado and Lopez 2006, Kwak and Kim 2002, Yalcin and Saatcioglu 2000)
For compressive behavior

$$f_c = f_c' \left[2\left(\frac{\varepsilon}{\varepsilon_0}\right) - \left(\frac{\varepsilon}{\varepsilon_0}\right)^2 \right] \qquad \varepsilon \le \varepsilon_0 \qquad (7a)$$

$$f_c = f_c' \left(1 - 0.15\left(\frac{\varepsilon - \varepsilon_0}{\varepsilon_{cu} - \varepsilon_0}\right)\right) \qquad \varepsilon_0 < \varepsilon \le \varepsilon_1 \qquad (7b)$$

$$f_c = 0.2 f_c' \qquad \varepsilon > \varepsilon_1 \qquad (7c)$$

Eq. 7(a) is Hognestad's model for concrete compressive behavior (Yalcin and Saatcioglu 2000). Eq. 7(b) is a linear function between peak stress and residual stress, Eq. 7(c) is residual stress that is assumed to be twenty percentage of the peak stress.
For tensile behavior

$$f_t = E_c \varepsilon \qquad \varepsilon \le \varepsilon_t \qquad (7d)$$

$$f_t = \lambda f_c' \left(1 - \frac{\varepsilon - \varepsilon_t}{\varepsilon_m - \varepsilon_t}\right) \qquad \varepsilon > \varepsilon_t \qquad (7e)$$

Eq. 7(d) is obtained from elastic behavior of concrete in the tensile region until the peak stress in tension; after this point softening behavior occurs. This behavior is usually simulated by a linear function (Assan 2002, Coronado and Lopez 2006, Kwak and Kim 2002, Yalcin and Saatcioglu

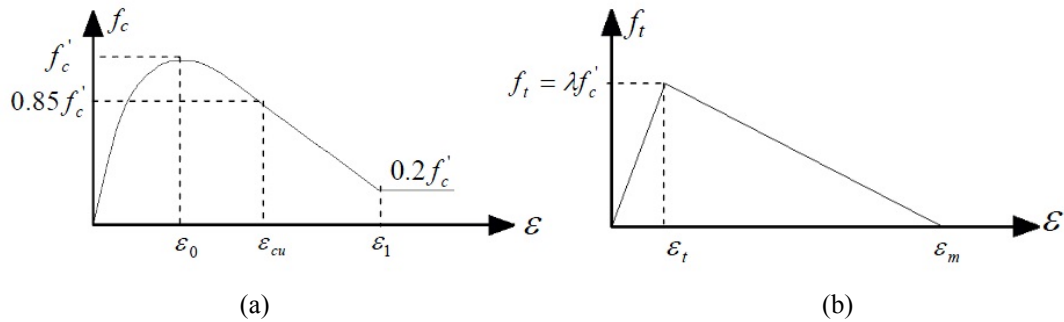(a)   (b)
Fig. 5(a) Compressive and (b) tensile behavior for concrete

2000).

Mostafaei *et al.* (2008) predicted the softening behavior by using an exponential function. In the other words, the softening behavior follows as an exponential function in terms of strain and the stress decrease by an exponential function. Here, a linear function (Eq. 7(e)) is assumed to determine the parameters of DSC for the softening behavior of concrete in tension. However, the DSC/HISS-CT model accounts nonlinear behavior of concrete in tensile region in terms of strain as the exponential function (Eq. (5) and Fig. 7). In Eq. (7), f_c' is 28-day compressive strength of concrete, $\varepsilon_0 = 0.002$, $\varepsilon_{cu} = 0.0038$, $\varepsilon_m = 10\varepsilon_t$, λ is varies between 0.1 to 0.25, as it normally occurs in experimental behavior (Park and Paulay 1975), E_c is modulus of elasticity of concrete, and ε_1, ε_t are shown in Fig. 5. Fig. 5(a) shows schematic plots of Eqs. 7(a) to 7(c) for compression, and Fig. 5(b) shows the plot for tension.

Eqs. 7(a) to 7(c) are used to construct compressive behavior of concrete with 28-days compressive strength, f_c' = 22.6, 24, 32 and 32.8 MPa, as shown in Fig. 6(a), in the positive quadrant; these values for f_c' are chosen to be consistent with concrete in later applications. Eqs. 7(d) and 7(e) are used to construct the tension behavior, as shown in Fig. 6(b), which is also shown in positive quadrant.

The DSC parameters are determined based on the constructed data in Fig. 6. Table 1 shows the parameters of the model for concrete in compression and tension. Ultimate disturbance, D_u=1 and atmospheric pressure, $p_a = 101.3 \ kPa$ are adopted. Details of determination of parameters are given by (Desai 2001).

It is noticeable that elastic modulus for the compressive strength equal to 22.6 MPa in Table 1 is not consistent with the generally accepted relation of Ec with the square root of compressive strength of concrete. It is usual practice in mechanics to determine the elastic modulus as the slope of the unloading curve or the slope at the origin of the stress-strain curve, for use in computer (finite element) analysis. Accordingly, for example, the elastic modulus equal to 36500 MPa is determined based on the stress-strain curve by Hognestad's (Yalcin and Saatcioglu 2000), Fig. 7. This elastic modulus was also observed by Vecchio and Shim (2004).
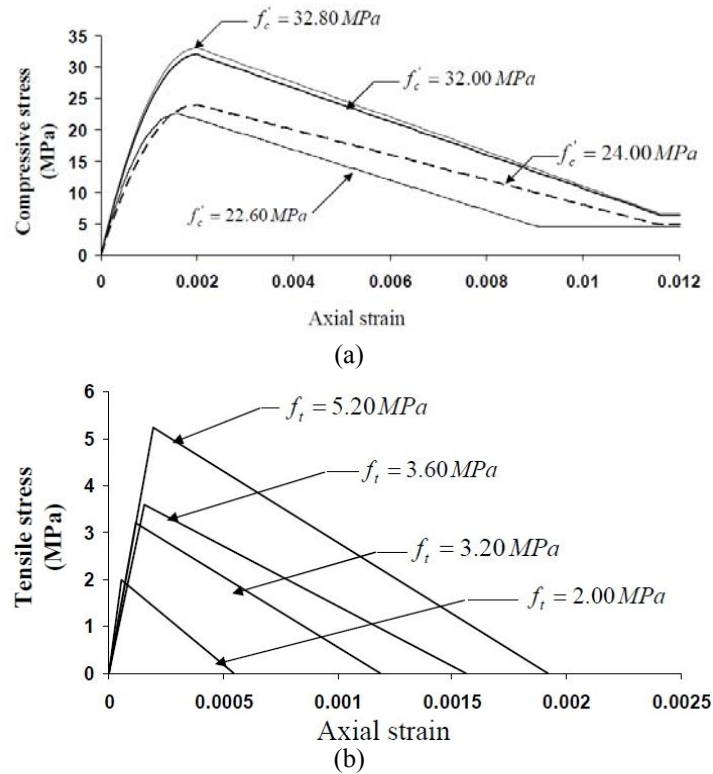
(a)

(b)

Fig. 6 (a) Compressive and (b) tensile behavior of concrete

Table 1 Parameters for DSC model

Compressive strength	Tensile strength	Kind of behavior	DSC Parameters/HISS Plasticity								Disturbance	
f'_c	f_t		E_c	υ	γ	β	n	R	$a1^*$ $1e9$	$\eta 1$	A	Z
24.00 (MPa)	3.60 (MPa)	Compression	23025.00 (MPa)	0.20	0.56	0.40	4.76	1.90	6.50	0.30	18269.00	1.93
		Tension	23025.00 (MPa)	0.20	0.09	0.40	4.76	1.95	6.50	0.30	32728.00	1.43
22.60 (MPa)	2.00 (MPa)	Compression	36500.00 (MPa)	0.20	0.56	0.40	4.76	1.90	6.50	0.30	18269.71	1.93
		Tension	36500.00 (MPa)	0.20	0.09	0.40	4.76	1.95	6.50	0.30	32728.45	1.20
32.00 (MPa)	3.20 (MPa)	Compression	27012.00 (MPa)	0.20	0.67	0.40	4.76	2.85	3.80	0.30	34891.00	2.06
		Tension	27012.00 (MPa)	0.20	0.06	0.40	4.76	2.85	2.00	0.30	27065.00	1.33
32.80 (MPa) (4770 psi)	5.20 (MPa)	Compression	24398.00 (MPa)	0.30	0.50	0.60	4.76	3.30	7.20	0.14	4339.00	1.77
		Tension	24398.00 (MPa)	0.30	0.03	0.50	4.76	5.23	2.00	0.11	62068.00	1.58

3.2 Specimen level validation

A computer program in the FORTRAN language is developed for the integration of Eq. (6); then it is used to validate the model at the specimen level using the parameters in Table 1. Fig. 7 shows comparison between predictions from the model and data for concrete with different 28-day compressive strengths as shown in Fig. 6. Note that such comparison for $f_c' = 32.8\,MPa$ is not shown in Fig. 7 due to its closeness to $f_c' = 32.0\,MPa$, and to avoid ambiguity in the figure.

It is clear from Fig. 7 that results from DSC model yields good agreement with the observed behavior based on the constructed data for compressive and tensile behavior with different peak stresses, different softening region slope and different residual stresses, Fig 7.

4. Applications

Numerical simulation of reinforced concrete structures and load-displacement responses are considered for concrete with different compressive strengths. Computer programs for two- and
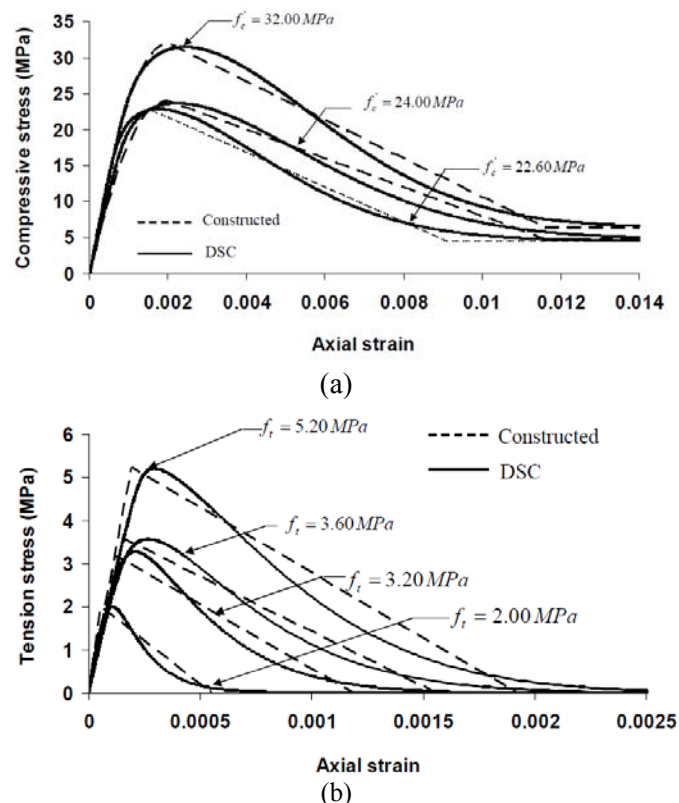

(a)

(b)

Fig. 7 Comparison between predictions and data for: (a) compressive and (b) tensile behavior

three- dimensional analysis (Desai 1998, 2000) with the DSC/HISS model have been developed and available; a computer code that allows the use of the HISS yield surface both for compression and tension in concrete has also been developed by Akhaveissy *et al.* (2009). Two nodded element with elastic perfectly plastic behavior is used for steel reinforcement. Results of the nonlinear computer analyses are compared with observed data in laboratory and load-displacement behavior obtained by using ANSYS software (Wolanski 2004); which is based on William and Warnke model (Willam and Warnke 1974) for concrete and elastic perfectly plastic model is assumed for the behavior of steel.

The iterative-incremental method with an initial stiffness scheme was used to analyze reinforced concrete structures. This method yielded accurate and convergent results for the problems considered. Both displacement and force convergences are evaluated. Convergence is obtained when the size of the residual force is less than the tolerance times a reference value. Here, the L2 norms in terms of residual force and the displacement are used for convergence. The L2 norm is the square root of the sum of the squares (SRSS) of the terms and is also called the Euclidean norm. The reference value for force control is the L2 norm of the increment of the force vector, and the reference value for displacement control is the L2 norm of the sum of the iterative displacements at each increment (Akhaveissy and Desai 2011). Hence, the solution time is about the same as the solution time by using ANSYS software; it may be noted that to our knowledge, ANSYS does not include unified models such as the DSC. As indicated in the forgoing, the DSC can allow for the post peak behavior; in fact, one of the advantages of the DSC is that includes entire behavior including pre-peak, peak and post- peak. As seen in Fig. 7, the model predicts the entire behavior with very good correlation with the constructed behavior, which is based on the observed behavior. In the subsequent examples, the load-displacement behavior does not show peak and softening. However, the stress-strain behavior, Fig. 7, includes the post-peak behavior. In other words, in many cases the load-displacement relation does not exhibit softening, while the stress-strain or constitutive behavior does.

The DSC/HISS model is capable of handling cyclic loading. It has been implemented in nonlinear finite element procedures which are used to solve a wide range of engineering problems including cyclic loading (Shao and Desai 2000, Park and Desai 2000, Park and Desai 2006); details are included in the text (Desai 2001). Future research would include the use of the model to analyze concrete structures subjected to cyclic loadings.

4.1 Simply-supported one-span beam

One-span beam tested by Buckhouse, and analyzed by Wolanski (2004) is considered. Fig. 8 shows the beam with length equal to 4724 mm (186 inch) under two concentrated loads at third points along the beam. Cross section of beam is 457×254 mm (18×10 inch). Supports are located at 76 mm (3 inch) from each end of the beam allowing a simply supported span of 4572 mm (15 ft). The mild steel flexural reinforcements are 3-#5 bars (area is equal to 600 mm^2) and shear reinforcements include #3 (area is 144 mm^2) U-stirrups. Cover for the rebar is set to 50 mm (2 inch) in all directions. The 28-days compressive strength of concrete is 32.8 MPa (4770 psi). Yield stress of bars is 413 MPa (60000 psi). Elastic modulus of steel reinforcements is 2×10^6 MPa (29×10^6 psi).

Half of beam is analyzed due to symmetry with 720 eight nodded isoparametric quadrilateral elements, 60 two nodded elements for longitudinal bars and 110 two nodded elements for U-stirrups. Fig. 9 shows boundary conditions and the finite element mesh.
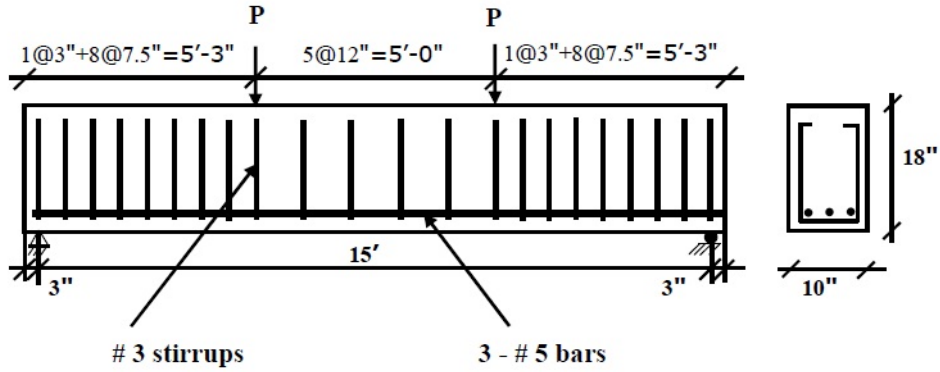
1 inch =2.54 cm; 1 ft= 30.50 cm
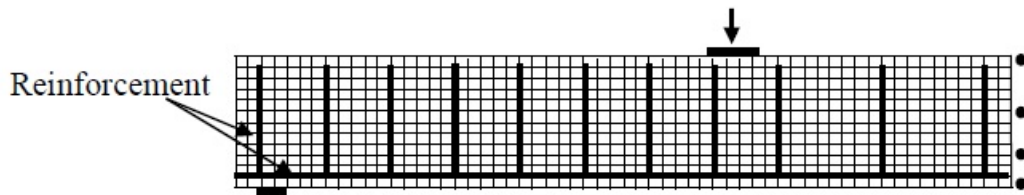Fig. 8 Details of buckhouse reinforced concrete beam (Wolanski 2004)

Fig. 9 Boundary conditions and finite element mesh for half of one-span beam, Fig.8
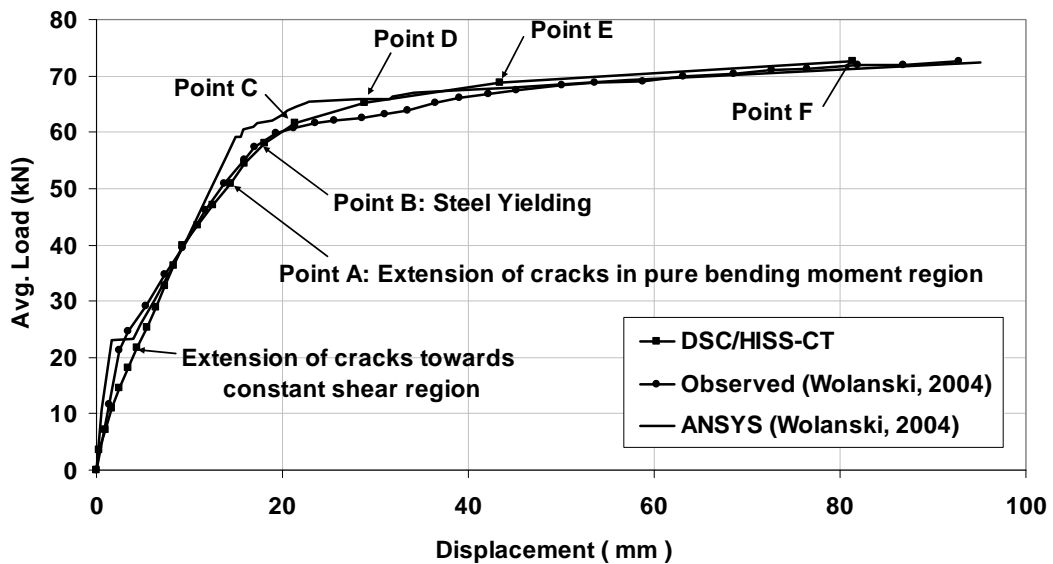

Fig. 10 Comparisons between DSC, observed and ANSYS results for Buckhouse beam

Calibrated parameters for compressive strength of concrete equal to 32.8 MPa (4770 psi) and tensile strength of concrete equal to 5.2 MPa (760 psi) are given in Table 1.

The beam is analyzed by using the DSC/HISS-CT model and results are compared with observed data and results obtained by using ANSYS. The load-displacement curve from the DSC model at middle of the beam is compared with results of ANSYS and the observed curve (Wolanski 2004), Fig. 10. It can be seen from Fig. 10 that the predictions from the DSC model compare very well with the test data and ANSYS results.

<u>Microcracks and fracture</u>

Wolanski (2004) presented that the vertical cracks first formed in the constant moment region, extended upward, and then out towards the constant shear region with eventual crushing of the concrete in constant moment region.

In the DSC the occurrence of microcracking leading to fracture and failure can be expressed in terms of the growth of disturbance, identified on the basis of test data (Desai 2001). According to Eqs. (4) and (5), D changes from 0.0 to 1.0. Disturbance equal to zero expresses that material is in fully relative intact (RI) state, and disturbance D= 1.0 expresses that material is in the fully adjusted (FA) state. In other words, the FA state indicates crushing or disintegration for compression or tension, respectively, after the peak stress. As stated before, microcracking for compression may initiate at stress = $0.3\sigma_p$ at $D \approx 0.001$ and it may occur at much lower D (=0.0001) for tension, Figs. 4 and 6. Then as stress and disturbance increase, microcracks grow and coalesce, and fracture may initiate at about D_c = 0.90, near the bottom, below the load, Fig. 11(a), corresponding to point A, Fig. 10. Then microcracks in extension grow further with loading, and fracture or failure zones extend at bottom and to the left of the load (when $D_c \geq 0.90$), Figs. 11(b), (c), (d), (f) and (g) at points B, C, D, E and F, respectively in Fig. 10. These trends are similar to Buckhouse's observations (Wolanski 2004) that extension cracks moved toward the constant shear region.

The growth and pattern of fracture or failure, Fig. 11, seem reasonable. For instance, Fig. 11(e) shows the crack patterns presented by Wolanski (2004) at point D, Fig. 10, using ANSYS. It can be seen that the cracks patterns computed using the DSC model at point D with the computed load = 65.27 kN, Fig. 11(d), are in general agreement with those predicted by ANSYS (Wolanski, 2004), at point D (load = 66.66 kN), Fig. 10. At the point F (Fig. 11(g)), the entire beam appears to reach disturbance of D_c = 0.90 and greater, which represents full failure. From the view point of design, the beam is considered to have failed somewhere between points C and E.

Fig. 11(a) shows extension of cracks in tension region of beam for point A in Fig. 10. At this loading, steel reinforcement exhibits linear behavior and maximum tensile stress in the reinforcements is 356 MPa (51696 psi) while yield stress in the reinforcement is 413 MPa for point B in Fig. 10, which shows beginning of reinforcement yielding. Buckhouse also expressed point B as the beginning of reinforcement yielding (Wolanski 2004).

The point F in Fig. 11(g) shows full failure or complete collapse. It should be noted that the spread of 'Full Failure' over almost the entire beam is not realistic. It may be noted, however, that the plots in Fig. 11, are for disturbance and not for the stress. Disturbance near the critical disturbance, Dc (=0.9), does not imply zero stress; in other words, there may be stresses in some zones in the beam at and after Dc. Hence, Fig. 12 shows distribution of shear stress and normal stress on beam for point F in Fig. 10.

(a)

(b)

Concentrated compression stress

Extension cracks

(c)

Compression Cracks

(d)

Extension Cracks

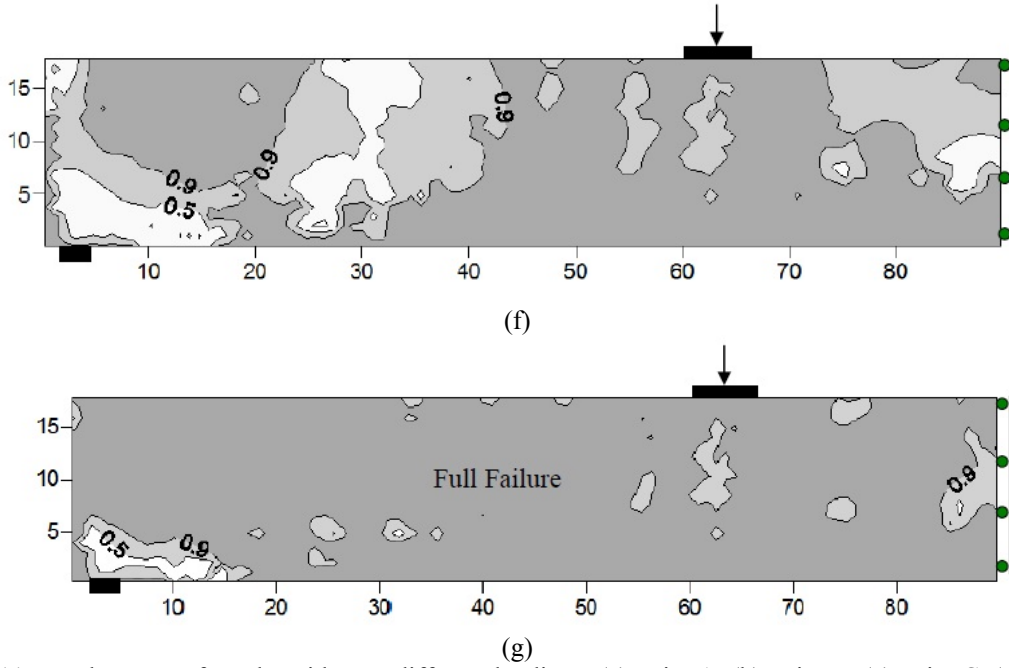Multiple cracks occurring

(e)

(f)

(g)

Fig. 11 Development of cracks with *D* at different loadings: (a) point A, (b) point B, (c) point C, (d) point D for load 65.27 kN, (e) point E for load 66.66 kN (Wolanski 2004), (f) point E and (g) point F at failure as in load-displacement curve in Fig. 10
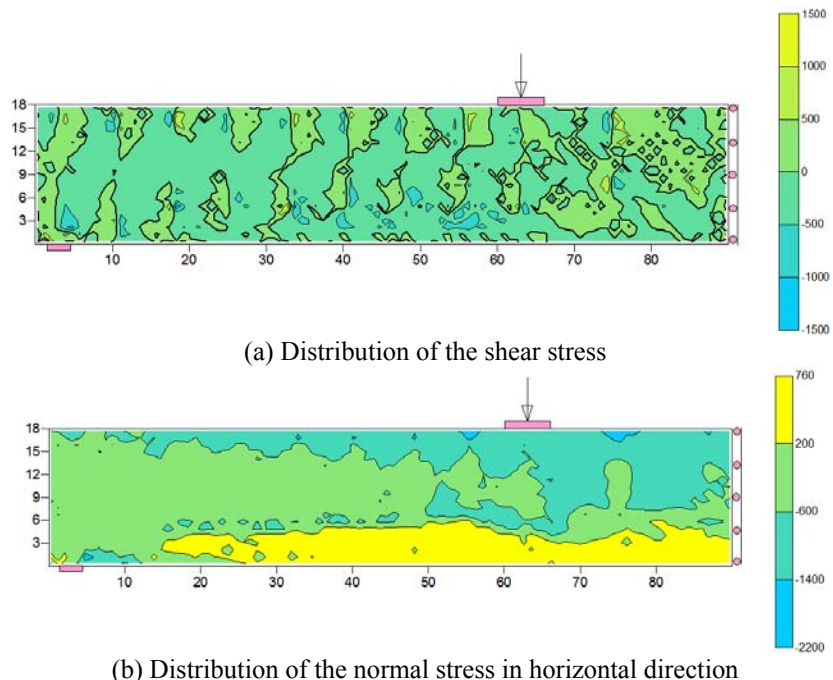

(a) Distribution of the shear stress

(b) Distribution of the normal stress in horizontal direction

Fig. 12 Distribution of stresses for point F in Fig. 10 (stresses in terms of psi)

4.2 Continuous beam

Half of the continuous beam, Fig. 13(a) tested by El-Refaie *et al.* (2003) is selected for analysis by use of DSC model. It was analyzed using ANSYS (Mostofinejad and Farahbod 2007) and predicted load-displacement curve was compared with observed data from laboratory by El-Refaie *et al.* (2003). Cross section of beam is 250 × 150 mm and total length of beam is 8500 mm. Longitudinal reinforcements are used in two layers with diameters of 8 and 20 mm. Diameter of stirrups is 6 mm. The compressive resistance of concrete is 24 MPa, the yield stress of bars with diameter 8 and 20 mm is 505 MPa and 510 MPa, respectively, and yield stress of bars with diameter of 6 mm is 308 MPa. Elastic modulus of steel reinforcements is 200 GPa.
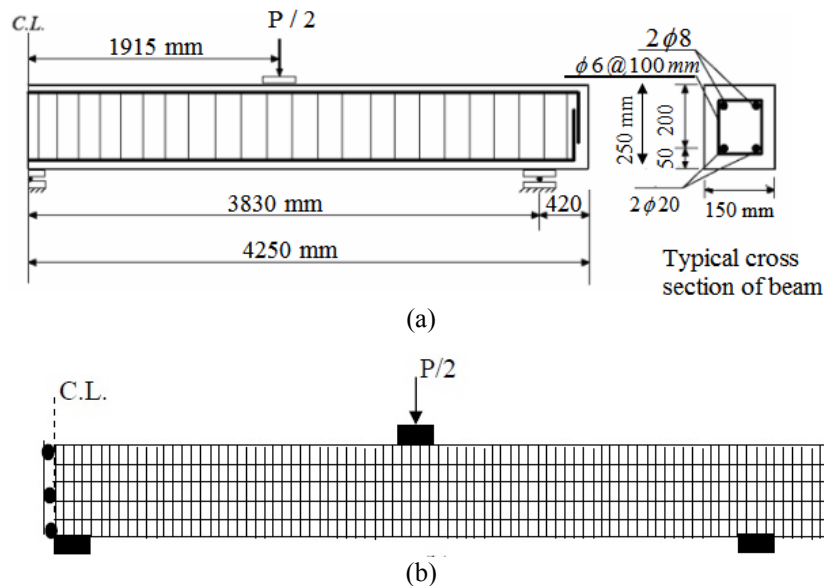

(a)

(b)

Fig. 13 (a) Details of continuous reinforced concrete beam and (b) finite element mesh
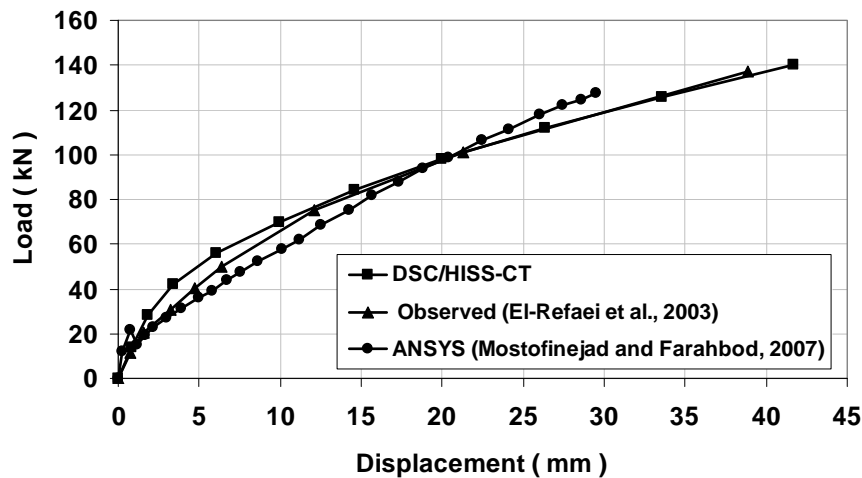

Fig. 14 Comparisons between DSC, observed and ANSYS results

Calibrated parameters for concrete with compressive strength equal to 24 MPa and tensile strength equal to 3.6 MPa are given in Table 1. Half of the beam is analyzed due to symmetry, Fig.13; the mesh includes 425 eight noded isoparametric quadrilateral elements, 170 two noded element for longitudinal bars and 42 two noded element for stirrups. Predicted load-displacement curve from the DSC is compared with results of ANSYS (Mostofinejad and Farahbod 2007) and observed curve in Fig. 14.

Both DSC and ANSYS yield essentially similar results and compare well with the observed data. However for loads lower than about 80 kN, DSC predicts higher loads than the observed, while ANSYS predicts lower load than the observed. The DSC model provides improved correlation with the test data in the ultimate region. The differences in the results are not high; however, they can be explained as follows. For the calibrated parameters at the specimen level with compressive strength equal to 24 MPa, the DSC model predicts stiffer behavior than constructed data in the initial region before compressive peak strength, Fig. 7(a). Therefore, the DSC model results show higher load at lower displacement. The difference between ANSYS and observed results may be due to the imprecision in the parameters obtained by using the trial and error procedure (Mostofinejad and Farahbod 2007).

4.3 Column

A column studied by Taylor *et al.* (1997) is selected for analyses using the DSC model. Fig. 15 shows the column with height (*L*) equal to 1000 mm under vertical and lateral concentrated loads at the top of the column. Cross section of column is 350 × 350 mm. The fixed support is located at bottom of the column. The mild steel flexural reinforcements are 8-#25.4 mm bars (area is equal to 4054 mm^2) and shear reinforcements including #10 mm stirrups. The 28-days compressive strength of concrete is 32 MPa. The yield stress of bars is 438 MPa. The elastic modulus of steel reinforcements is 200 GPa.

Load-displacement curve from the laboratory was obtained in terms of lateral load versus lateral displacement (Taylor *et al.* 1997). The column was analyzed also by Yalcin and Saatcioglu (2000). Fig. 16 shows finite element mesh for the DSC model; it contains 140 eight noded isoparametric quadrilateral elements with plane stress behavior, 60 two noded elements for
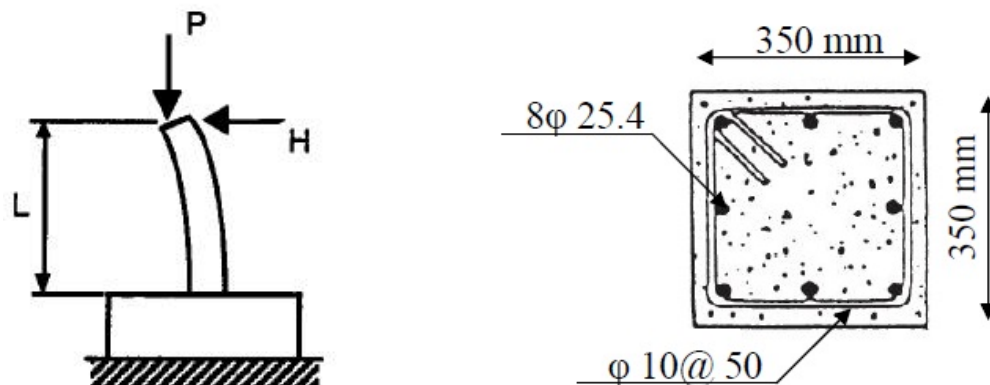

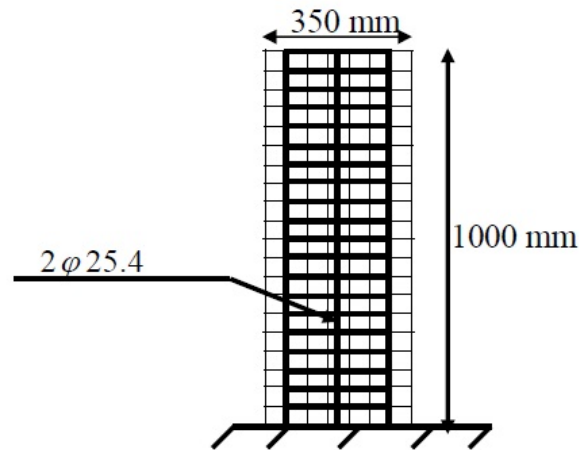Fig. 15 Details of reinforced concrete column

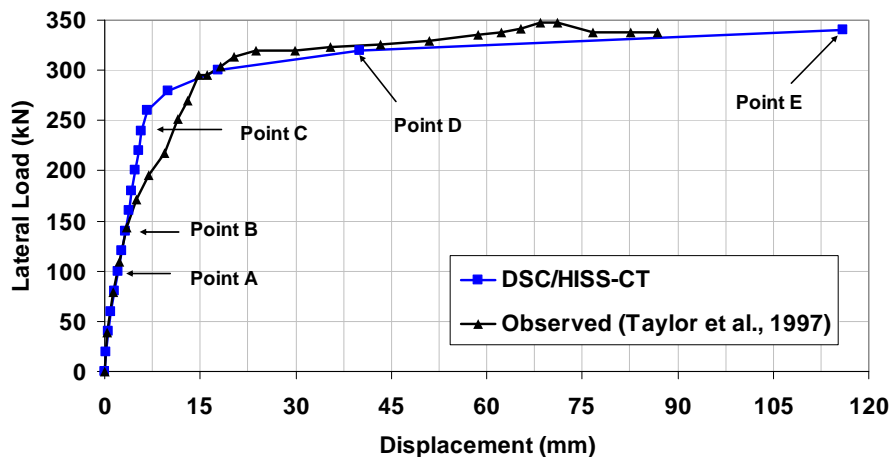Fig. 16 Finite element mesh for analysis of column

Fig. 17 Comparisons between DSC and observed results for reinforcement concrete column

longitudinal bars and 100 two noded elements for stirrups.

The parameters for DSC model for 28-days compressive strength of concrete equal to 32 MPa and tensile strength of concrete equal to 3.2 MPa are given in Table 1. Lateral load-displacement curve at the top of the column based on finite element analysis using the DSC/HISS-CT model is compared with the test data in Fig. 17. It shows good correlation between the DSC predictions and observed data; the correlation in the ultimate region is particularly very good.

As mentioned in section 2.2.1 Disturbance, microcracking may initiate at D =0.001 and 0.0001 for compression and tension, respectively. Then, fracture may initiate around D_c= 0.90. Fig. 18 shows development of D which indicates the initiation and growth of cracks. Figs 18 (a), (b), (c)
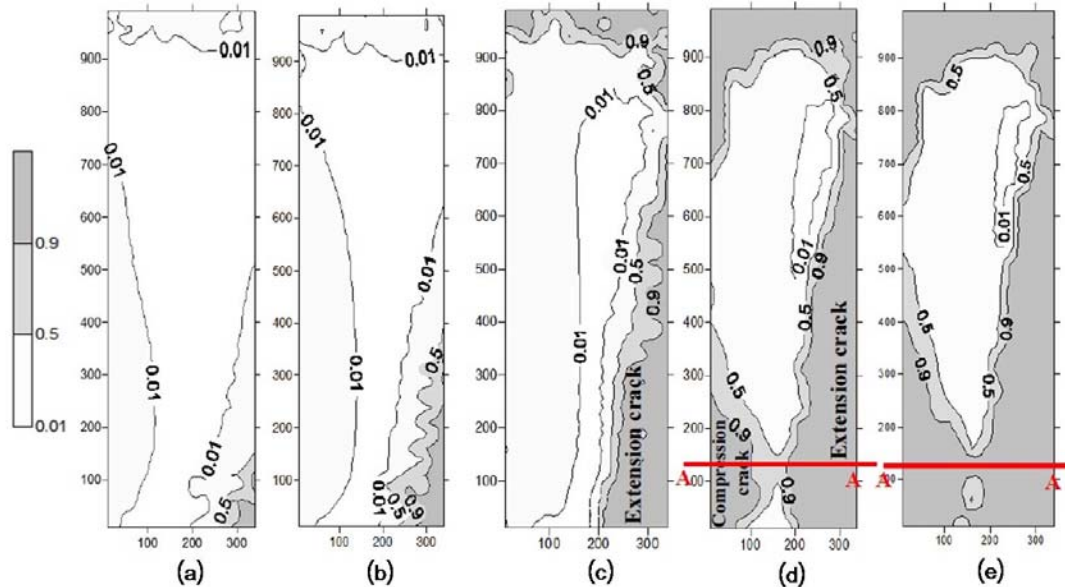
Fig. 18 Growth of cracks with *D* for reinforced concrete beam-column: (a) point A, (b) point B, (c) point C, (d) point D and (e) point E in Fig. 17

and (d) show crack patterns for points A, B, C and D in Fig. 17, respectively. In the extension zone of the column, cracks may initiate and grow, Fig. 18(a) when *D*= 0.0001 has been exceeded, and fracture would occur when D_c = 0.90 or greater has been reached, Fig. 18(d). Similarly cracks in the compression zone can initiate and grow to fractures when D_c = 0.9 or greater occurs, Fig. 18(d). The displacement for the increment of load from point D to E is about 75 mm; which is considered to be very high. The column can be considered to have failed between points D and E. Hence, the computations were terminated at the load of 340 kN, i.e., point E. Cross section A in Fig. 18(e) shows also full failure. In the other words, the cross section indicates the plastic hinge. Hence, the column can be considered to have failed under load corresponding to the state of failure in Fig. 18(e).

4.4 Simply-supported one-span beam with three layer bars

RC beam specimens A1 and A3 tested by Vecchio and Shim (2004) were selected for analysis by Saritas and Filippou (2009). The predicted load-displacement curve by Saritas and Filippou (2009) for beam A3 correlate with test data but the predicted result for beam A1 is different with test data. Therefore, beam A1 is considered in here. The geometric properties and reinforcement details are shown in Fig. 19. The compressive strength of concrete, Young modulus of concrete and the tensile strength of concrete were reported 22.6 MPa, 36500 MPa and 2.37 MPa, respectively by Vecchio and Shim (2004). Table 2 shows material properties of the beam.

The parameters for DSC/HISS-CT model for 28-days the compressive strength of concrete equal to 22.6 MPa and tensile strength of concrete equal to 2 MPa are given in Table 1. The load-
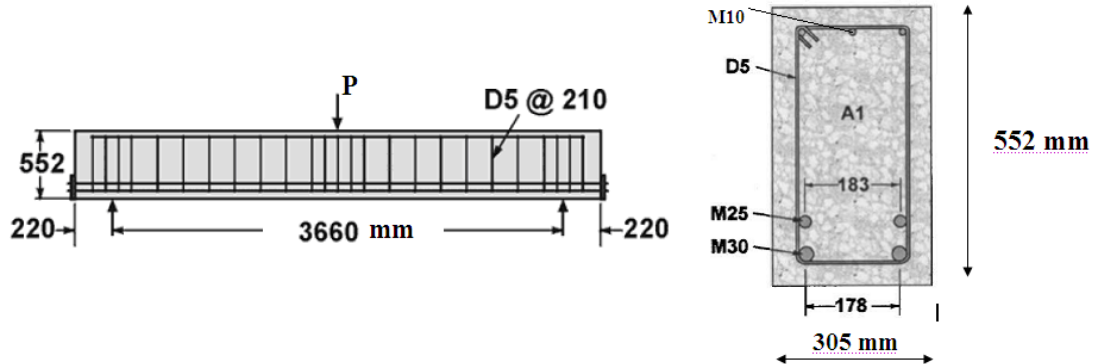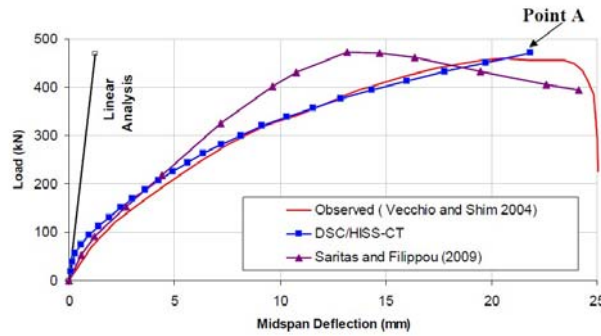
Fig. 19 Details of reinforcement concrete beam

Fig. 20 The comparison between predicted load-deflection curve and test data

Table 2 Material properties of beam

Concrete		
f_c' (MPa)	f_t (MPa)	E (MPa)
22.6	2.37	36500
Reinforcement					

Bar size	Diameter (mm)	Area (mm²)	F_y (MPa)	F_u (MPa)	E (MPa)
M10	11.3	100	315	460	200000
M25	25.2	500	440	615	210000
M30	29.9	700	436	700	200000
D5	6.4	33.2	600	649	200000

displacement curve at center of the beam based on finite element analysis using the DSC model is compared with the test data in Fig. 20.

Fig. 20 shows very high correlation between the DSC predictions and observed data; the correlation in the ultimate region is particularly very good, but the predicted result by Saritas and
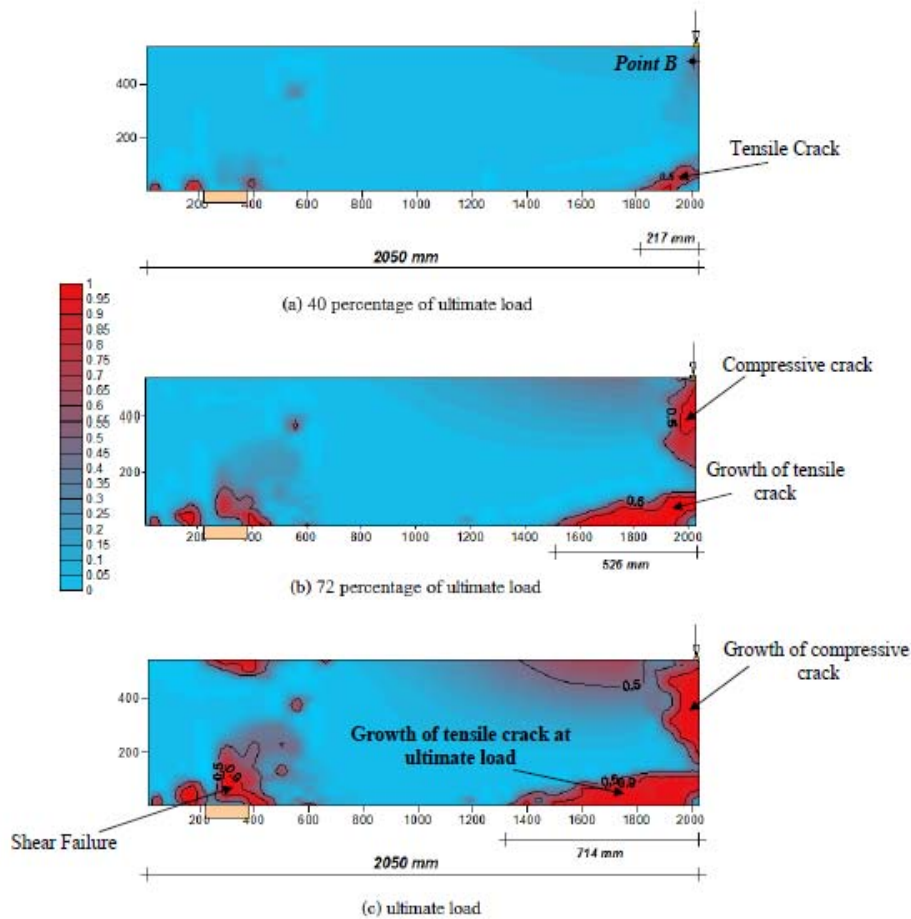
Fig. 21 Growth of cracks with *D* for different load levels: (a) 40 percentage of ultimate load, (b) 72 percentage of ultimate load and (c) ultimate load point A in Fig. 20

Filippou (2009) is not in accordance with the test data and DSC/HISS-CT. The analysis by DSC/HISS-CT model ***did not converge*** after ultimate load (point A from Fig. 20). In the other words, the beam failed at point A from Fig. 20. The process of failure for the beam by use of the model is expressed in Fig. 21.

Fig. 21 shows disturbance parameter to express the failure process of the beam for different load levels. Fig. 21(a) shows tensile crack at mid-span of beam due to maximum bending moment. The tensile crack grows with increase of the load and the crushing occurs due to compressive normal stress at top of the section, Fig. 21(b). Failure occurs due to the extension of the tensile cracks and crushing due to compressive stress at mid-span of the beam and also increasing of shear stress with yielding stirrups close to the support. Fig. 22 shows the shear stress versus the shear strain at closest gauss point to the mid-span of the beam with coordinate (x=2028 mm, y=494 mm), see point B from Fig. 21(a). The predicted tensile principal stress by DSC/HISS-CT for point B from Fig. 21 (a) in accordance with point C in Fig. 22 is 2.25 MPa while the tensile strength was 2
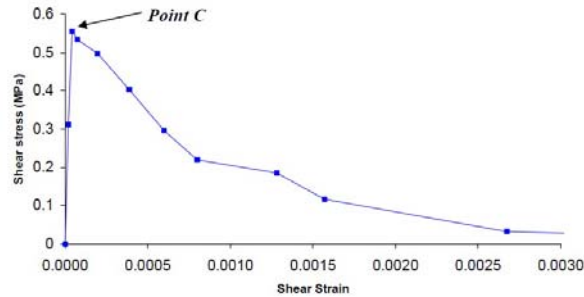
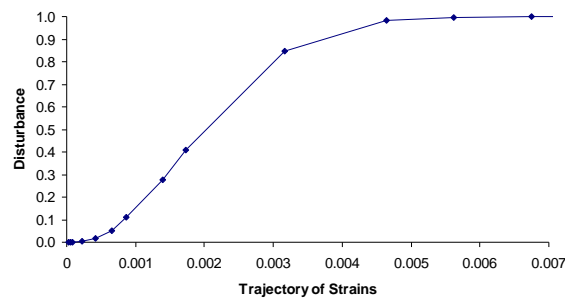Fig. 22 The shear strain versus shear stress at the mid-span of the beam

Fig. 23 Disturbance at mid-span of the beam for the point B, Fig. 21(a)

MPa, Table 1. Therefore point B from Fig. 21(a) has been cracked as the tensile principal stress 2.25 MPa is greater than the tensile strength 2 MPa. Then disturbance parameter, *D*, grow and it will be beginning of the softening behavior of the shear stress–shear strain curve. In the other words, cracks start when the tensile principal stress in principal stress space reaches to the tensile strength of the material. The disturbance parameter for this point, point B from Fig. 21(a), is shown in Fig. 23. It expresses amount of the disturbance parameter equal to 0.9 occurs at the strain 0.0035 approximately and amount of the shear stress at this strain from Fig. 22 is about 0.021 MPa, about 5% of the ultimate shear stress.

5. Comments

ANSYS is considered to be a powerful program to analyze different structures, and uses model of William and Warnke (1974) for analysis of concrete behavior. Determination of model parameters in ANSYS is based on error reduction by iteration (trial and error) to fit the load-displacement curve. Parameters of DSC/HISS-CT model are calibrated based directly on the actual (e.g. measured stress-strain) behavior of the material, e.g. by using Eqs. (1), (2), (4) and (5). Therefore, analysis by DSC/HISS-CT model is considered to be more reliable compared to the model used in ANSYS.

Often models such as Willam and Warnke available in ANSYS are for specific behavior like failure. However, materials under loading may exhibit combined behavior such as elastic, plastic, continuous yield, failure and softening. Then the proposed DSC/HISS-CT model which is unified

and hierarchical can provide for such combined behavior including as elastic, plastic, continuous yield, microcracking leading to fracture, failure and softening within the same framework.

6. Conclusions

The nonlinear finite element method with eight noded isoparametric quadrilateral elements for concrete and two noded elements for steel used for prediction of the behavior of reinforced concrete structures. The disturbed state concept (DSC) with the modified hierarchical single surface (HISS-CT) plasticity model was used to characterize the yield behavior in compressive and tensile behavior of concrete. Such a model, DSC/HISS-CT that allows for both compressive and tensile yields is used for the first time in this paper. The model can account for microcracking in concrete leading to softening and fracture. The elastic perfectly plastic behavior was assumed to model the steel reinforcement. The DSC approach possesses a number of advantages compared to other available models. Its hierarchical property allows the user to adopt model of increasing complexity such as elastic, plastic, viscoplastic, microcracking leading to fracture, degradation and softening, and healing, with the same mathematical framework. The HISS-CT plasticity model involves a two continuous yield surface thereby avoiding computational difficulties for discontinuous or multiple surfaces models

The DSC/HISS-CT model for concrete has been validated at the specimen level. It is applied successfully for a number of reinforced concrete structures. The computer predictions correlate very well with test data as well as with predictions reported by using the commonly employed ANSYS code. As explained above, the DSC model is general and unified; hence, it possesses certain advantages compared to other available model that are developed for specific behavioral aspects. Hence, the DSC/HISS-CT model can be considered to provide improvement in modeling various behavioral features of concrete such as elastic, plastic deformations, microcracking leading to fracture and softening.

The parameters for the DSC model can be determined approximately from triaxial tests. However, a number (about five) of test data under various stress paths, e.g. compression, extension and simple shear are desirable for more accurate determination of the parameters to include the three-dimensional effects in the DSC model. Hence, non availability of such tests can be considered to be a limitation of the DSC model. For general reinforced concrete problems and for future research, detailed triaxial and multiaxial tests for concrete under various practical stress paths, and shear tests for interfaces between concrete and reinforcement could be performed; the latter would account for possible relative motions between concrete and reinforcement. The same mathematical framework of the DSC model can be used for both concrete and interfaces.

References

Akhaveissy, A.H., Desai, C.S., Sadrnejad, S.A. and Shakib, H. (2009), "Implementation and comparison of generalized plasticity and disturbed state concept for load-deformation behavior of foundation", *Sci. Iran. J. Trans. A Civil Eng.*, **16**, 189-198.

Assan, A.E. (2002), "Nonlinear analysis of reinforced concrete cylindrical shells", *Comput. Struct.*, **80**(27-30), 2177-2184.

Bathe, K.J. (1996), *Finite element procedures*, Prentice-Hall, Inc., Upper Saddle River, New Jersey, USA.

Bazant, Z.P. and Shieh, C.L. (1978), "Endochronic model for nonlinear triaxial behavior of concrete", *Nucl. Eng. Des.,* **47**(2), 305-315.

Bazant, Z.P. and Luzio, G.D. (2004), "Nonlocal microplane model with strain-softening yield limits", *Int. J. Solids Struct.*, **41**(24-25), 7209-7240.

Carol, I., Part, P. and Bazant, Z.P. (1992), "New Explicit microplane model for concrete: theoretical aspects and numerical implementation", *Int. J. Solids Struct.*, **29**(9), 1173-1191.

Cervera, M., Hinton, E. and Hassan, O. (1987), "Nonlinear analysis of reinforced concrete plate and shell structures using 20-noded isoparametric brick elements", *Comput. Struct.*, **25**(6), 845-869.

Coronado, C.A. and Lopez, M.M. (2006), "Sensitivity analysis of reinforced concrete beams strengthened with FRP laminates", *Cement Concrete Comp.*, **28**(1), 102-114.

Desai, C.S. (1998), *DSC-SST2D code for two-dimensional static, repetitive and dynamic analysis: User's Manuals I to III*, Tucson, AZ, USA.

Desai, C.S. (2000), *DSC-SST3D code for three-dimensional coupled repetitive and dynamic analysis*, Tucson, AZ, USA.

Desai, C.S. (2001), *Mechanics of materials and interfaces: the disturbed state concept*, CRC Press, Boca Raton, Florida, U.S.A.

Desai, C.S. (2002), "Mechanistic pavement analysis and design using unified material and computer models", *Proc. 3rd Intl. Symposium on 3D Finite Elements for Pavement Analysis, Design and Research*, Amsterdam, The Netherlands.

Desai, C.S. (2007), "Unified DSC constitutive model for pavement materials with numerical implementation", *Int. J. Geomech. ASCE*, **7**(2), 83-101.

Desai, C.S. and Salami, M.R. (1987), "A constitutive model for rocks", *J. Geotech. Eng. ASCE*, **113**, 407-423.

Desai, C.S., Somasundaram, S. and Frantziskonis, G. (1986), "A hierarchical approach for constitutive modeling of geologic materials", *Int. J. Numer. Anal. Meth. Geomech.*, **10**(3), 225-257.

Desai, C.S. and Toth, J. (1996), "Disturbed state constitutive modelling based on stress-strain and nondestructive behavior", *Int. J. Solids Struct.*, **33**(11), 1619-1650.

El-Refaie, S.A., Ashour, A.F. and Garrity, S.W. (2003), "Sagging and hogging strengthening of continuous reinforced concrete beams using carbon fiber-reinforced polymer sheets", *ACI Struct. J.*, **100**(4), 446-453.

Kachanov, L.M. (1986), *Introduction to continuum damage mechanics*, Martinus Nijhoff Publishers, Dordrecht, The Netherlands.

Kwak, H.G. and Kim, S.P. (2002), "Nonlinear analysis of RC beams based on moment-curvature relation", *Comput. Struct.*, **80**(7-8), 615-628.

Mostafaei, H., Vecchio, F.J. and Kabeyasawa, T. (2008), "Nonlinear displacement-based response prediction of reinforced concrete columns", *Eng. Struct.*, **30**(9), 2436-2447.

Mostofinejad, D. and Farahbod, F. (2007), "Parametric study on moment redistribution in continuous RC beams using ductility demand and ductility capacity concepts", *Iran. J. Sci. Technol. Trans. B Eng.*, **31**(5), 459-471.

Park, I.J. and Desai, C.S. (2000), "Cyclic behavior and liquefaction of sand using disturbed state concept", *J. Geotech. Geoenviron. Eng. ASCE*, **126**(9), 834-846.

Park, R. and Paulay, T. (1975), *Reinforced concrete structures*, John Wiley & Sons, Inc. Singapore.

Pradhan, S.K. and Desai, C.S. (2006), "DSC model for soil and interface including liquefaction and prediction of centrifuge test", *J. Geotech. Geoenviron. Eng. ASCE*, **132**(2), 214-222.

Salami, M.R. and Desai, C.S. (1990), "Constitutive modeling including multiaxial testing for plain concrete under low confining pressure", *J. Mater. Am. Concrete Inst.*, **87**(3), 228-236.

Saritas, A. and Filippou, Filip C. (2009), "Numerical integration of a class of 3d plastic-damage concrete models and condensation of 3d stress-strain relations for use in beam finite elements", *Eng. Struct.*, **31**(10), 2327-2336.

Shao, C. and Desai, C.S. (2000), "Implementation of DSC model and application for analysis of filed pile tests under cyclic loading", *Int. J. Numer. Anal. Meth. Geomech.*, **24**(6), 601-624.

Taylor, A.W., Kuo, C., Wellenius, K. and Chung, D. (1997), *A summary of cyclic lateral load test on rectangular reinforced concrete columns*, NISTIR 5984, National Institute of Standards and Technology, Gaithersburg, Maryland.

Vecchio, F.J. and Shim, W. (2004), "Experimental and analytical reexamination of classic concrete beam tests", *J. Struct. Eng.-ASCE*, **130**(3), 460-469.

Weibull, W.A. (1951), "A statistical distribution function of wide applicability", *Appl. Mech.*, **18**, 293-297.

Willam, K.J. and Warnke, E.P. (1974), "Constitutive model for triaxial behavior of concrete", Seminar on Concrete Structure Subjected to Triaxial Stress, *International Association of Bridge and Structural Engineering Conference*, Bergamo, Italy.

Willam, K. and Tanabe, T.A. (2001), *Finite element analysis of reinforced concrete structures*, American Concrete Institute, Farmington Hills, MI.

Wolanski, A.J. (2004), *Flexural behavior of reinforced and prestressed concrete beams using finite element analysis*, Master's Thesis, Marquette University, Milwaukee, Wisconsin.

Yalcin, C. and Saatcioglu, M. (2000), "Inelastic analysis of reinforced concrete columns", *Comput. Struct.*, **77**(5), 539-555.

Zienkiewicz, O.C., Valliapan, S. and King, I.P. (1968), "Stress analysis of rock as a no tension material", *Geotech.*, **18**(1), 56-66.

CC

Notations

C^e = Elastic matrix;

D = Disturbance parameter;

E_c = Elastic modulus of concrete (MPa);

F = Yield function;

f_t = Tensile strength of concrete (MPa);

f_c' = 28-days compressive strength of concrete (MPa);

p_a = Atmospheric pressure (kPa);

Q = Potential function;

$\varepsilon_0 = 0.002$;

$\varepsilon_{cu} = 0.0038$;

ζ = Trajectory of plastic strains;

υ = Poisson's ratio; and

φ = Diameter of steel bar (mm).